Chapter 6

Emissivity Tests in Reverberation Chambers

6.1. Introduction

Chapter 5 was devoted to measurements of radiated immunity, which are certainly at the origin of the current upsurge the use of reverberation chambers in several industrial sectors. However, the first research studies on this subject [COR 76] had as an objective the measurement of microwave radiations. Indeed, the stochastic nature of the field was first postulated during these initial studies. This stochastic behavior is potentially produced by an electromagnetic cavity of large dimension compared to the wavelength, in mode stirring operation. We then quickly noticed that the reverberation chamber behaved in such a way that the intrinsic directivity of the radiating element placed inside was mostly hidden. The standing wave regime present in the cavity strongly contributes to hide this directivity and the stirring operation strengthens this property. Therefore, an antenna also set in the enclosure enables us to intercept an electromagnetic signal, whose amplitude is directly linked to the radiated power supplied by the transmitter.

This property is at the origin of the use of reverberation chambers for the determination of the total radiated power of a device under test. The total radiated power can notably enable us to characterize the unintentional radiation of a device, in order to evaluate its interference level. In this chapter we will take a more particular look at the applicable methods of quantifying of this magnitude. However, the total radiated power does not give any indication of the favored radiation directions, and consequently of the maximum available power received by a device located in the environment. This information must be rebuilt, in order to carry out a

complete risk analysis of electromagnetic compatibility. It is thus useful to describe the extent to which the total radiated power, which is evaluated in reverberation chambers, can be linked to the measurement of the maximum electric field radiated at a normalized distance from a device. This is usually the criterion used to quantify the radiated emissivity.

Beyond the measurement of the total radiated power, the different power balances, which can be established in a reverberation chamber, lead quite naturally to considering the extension of the applications of such chambers to the characterization of the antenna performances. The last part of this chapter is devoted to the evaluation techniques of the antenna performances, such as the efficiency measurement, the measurement of the diversity gain, notably during the use of transmission or reception devices with several antennas.

However, we start this chapter by recalling a few notions on electromagnetic radiation and antennas, which will be potentially useful later on.

6.2. A few notions on electromagnetic radiation and antennas

6.2.1. *Origin of electromagnetic radiation*

The source of electromagnetic radiation is intrinsically the modification of the flow speed of electric charges in space, i.e. variation of the current. This variation can come from the coupling of an alternative energy source. However, in continuous supply regime, the speed variation can come from the geometrical form of the radiating element. As an example, the curvature or the end of an electrically conducting wire can be at the origin of the electromagnetic radiation. The combination of these two effects is quite frequent. The radiation of an electric dipole is favored by its coupling to an alternative source (mainly if it is a continuous wave source adjusted to the tuning frequency of the dipole) and mainly occurs at the extremities [BAL 05].

6.2.2. *Properties of the electromagnetic field at a distance from the radiation source*

The radiated field is first closely dependent on the nature of the antenna in a restricted geographical zone surrounding this antenna. In the proximity zone, also called the reactive zone of the near-field, the electromagnetic field lines remain partly shut on the transmitting antenna. They represent the energy stored in a *capacitive* form for an electric antenna, or in an *inductive* form for a magnetic antenna.

By moving away from this zone, we enter the radiated near-field zone, where the field lines no longer close themselves on the antenna. They detach themselves from it while closing on themselves due to the spatiotemporal alternation of the positive and negative charges, which are introduced by the alternative coupling source. The electromagnetic wave is then propagated at a distance from the antenna. However, the angular field distribution varies with the distance of the antenna up until we reach the far-field zone, where the angular distribution no longer varies.

Analysis of the solution properties of Maxwell's equations enables us to establish the approximate limits of these three respective zones for an antenna whose maximum dimension in any direction of space is noted D. Figure 6.1 symbolizes this progressive structuring of the field, as a function of the distance between the observation point and the center of the reference mark, which is located on the antenna.

It thus appears that the dimension of the antenna and more precisely the ratio between this dimension and the wavelength plays an important part in the analysis of the field distribution at a distance from this antenna. We can distinguish the Rayleigh region, for which the electromagnetic field is mainly of a reactive nature. The boundary of the $R_{Ray\text{-}Fre}$ radius corresponds to the limit between the Rayleigh region and the Fresnel region, for which the electromagnetic field is comparable to a wave that propagates the infinity of space. In this zone and beyond, the total radiated power towards the outside of this area remains constant, whatever the radius of the considered sphere. However, the angular distribution of the electromagnetic field changes because of the observation distance, and the radial components of the field are still of significant amplitude.

The $R_{Ray\text{-}Fre}$ radius is estimated at $0.62\sqrt{D^3/\lambda}$ or at $\lambda/(2\pi)$, if the source is very small with regard to the wavelength. The Fraunhofer region corresponds to the far-field zone, for which the electromagnetic field has common properties with all the radiation sources. The angular distribution of the electromagnetic field does not vary with the observation distance. The radial components of the electromagnetic field almost disappear.

The electric field vector is perpendicular to the magnetic field vector. They are also both perpendicular to the vector fixing the propagation direction (from the source to the observation point). The ratio of the modulus of the electric field and of the magnetic field is constant and equal to the wave impedance of the propagation medium. In the case where the environment is air, we admit that this impedance is $\sqrt{\mu_0/\varepsilon_0} = 120\pi\Omega$. Finally, the electric field (as well as the magnetic field) decreases in inverse proportion with the distance to the source.

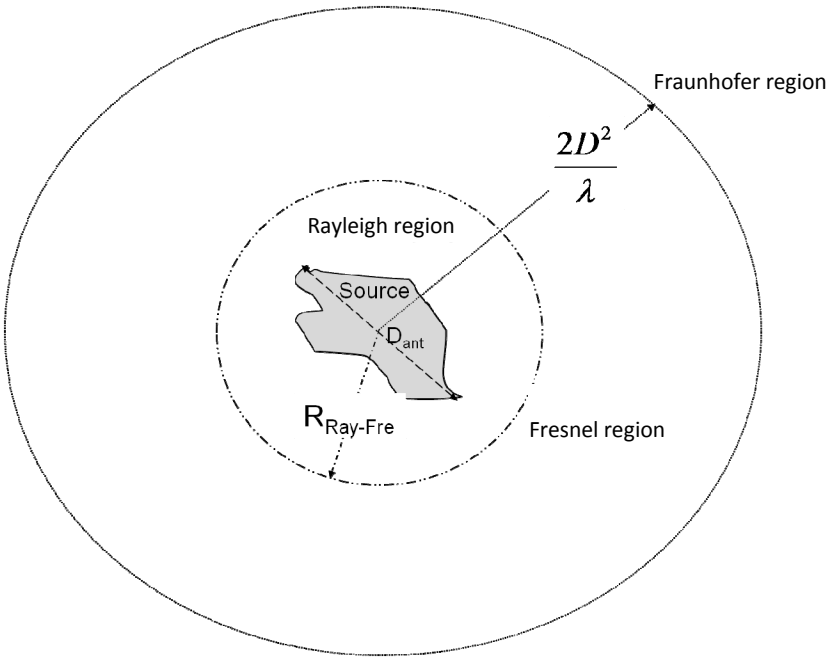

Figure 6.1. *Electromagnetic radiation zones*

In reverberation chambers, the interactions between antennas or between an antenna and a radiating element are, most of the time, located in the far-field (Fraunhofer region) or, failing that, in the Fresnel region. This is partly explained by the fact that a reverberation cavity has larger dimensions than the wavelength. It thus leads to the installation of a reception device at a sufficient distance from the transmission source. Otherwise, the interpretation of the results is particularly tricky in relation to the estimate of the total radiated power which is not preserved in the Rayleigh region. The coupling between the transmitting and receiving antennas is also involved in this context.

6.2.3. *Intensity and directivity of the electromagnetic radiation*

The intensity and directivity of the electromagnetic radiation are defined in the far-field zone or in the Fraunhofer region, where the angular distribution of the radiation is invariant. We define a spherical coordinate system (O,r,θ,φ), whose center O is located at the locus of the radiation source. θ and φ respectively denote the elevation angle and the azimuth angle. The radiation intensity at a distance r, for

an observation point located in the Fraunhofer region, is the radiated power at this point per unit of solid angle of the sphere of radius *r*. Mathematically this gives:

$$U(\theta,\phi) = r^2 dP_{rad}(r,\theta,\phi) \qquad Watt / steradian \qquad [6.1]$$

$dP_{rad}(r,\theta,\varphi)$ is the power density in Watt/m^2 at this point. In the Fraunhofer region, this power density is connected to the amplitude of the electric field and to the wave impedance by:

$$dP_{rad}(r,\theta,\varphi) = \frac{\left|E(r,\theta,\varphi)\right|^2}{2Z_w} \qquad [6.2]$$

where *E* is the electric field at the considered point. Because of the previously mentioned properties, it can be formulated as:

$$E(r,\theta,\varphi) = C(\theta,\varphi)\frac{\exp(-jkr)}{r} \qquad [6.3]$$

In this expression C represents an unknown constant of the problem whose value depends on the total radiated power by the transmitting antenna. We thus check that the radiation intensity is independent of the choice of *r*.

In theory, the electromagnetic radiation can be of the same density, whatever the observation direction. This radiation is then said to be isotropic. The radiation intensity of an isotropic source U_0 is given by:

$$U_0 = \frac{P_{rad}}{4\pi} \qquad [6.4]$$

where P_{rad} is the total radiated power by the source.

However, in practice, a source of electromagnetic radiation is not isotropic, because it does not have the required symmetry properties. By misnomer, we call an antenna with rotation symmetry around an axis and generating a radiation of isotropic nature following a perpendicular plane to this symmetry axis an isotropic antenna.

Therefore, the introduction of the directivity notion is essential to characterize the preferential radiation directions (or the opposite) of the source. The directivity in one direction (θ,φ) is the ratio existing between the radiation intensity in this direction and the intensity that would have been observed in the hypothesis of an isotropic radiation. This is conveyed by:

$$D(\theta,\varphi) = \frac{U(\theta,\varphi)}{U_0} = \frac{4\pi U(\theta,\varphi)}{P_{rad}} \qquad [6.5]$$

6.2.4. *Polarization and partial directivities*

Electromagnetic radiation is represented by vector fields. The polarization of the field is defined with reference to the direction taken by the electric field and is also defined in the meaning of the far-field.

Polarization depends on the geometry and on the excitation mode of the radiating element. Thus, an element with a current that is collinear to the *Oz* direction and is of dimension $dl << \lambda$ (see Figure 6.2) will be at the origin of a polarized electric field following $\vec{\theta}$, according to expression [6.6].

In this expression, the field is defined by the constant, noted C_S, dependent on the amplitude of the excitation current:

$$\vec{E} = C_S \sin\theta\vec{\theta} \qquad [6.6]$$

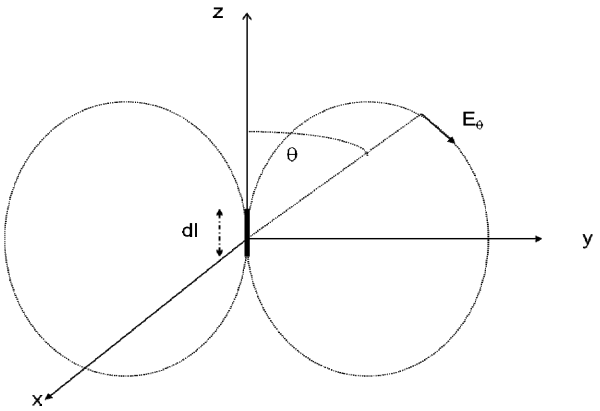

Figure 6.2. *Polarization example of the field along θ for a small current element aligned along Oz*

In the more general case, the electric field appearing in expression [6.3] is written:

$$\vec{E}(r,\theta,\varphi) = E_\theta \vec{\theta} + E_\varphi \vec{\varphi} \qquad [6.7]$$

It is then possible to define the partial radiation directivities according to the θ and φ elementary angles. In this way we will define the partial directivity according to the θ angle as the ratio of the radiation intensity in one given direction (θ,φ) and in this polarization, at the radiation intensity that would have been produced by an isotropic source:

$$D_\theta(\theta,\varphi) = \frac{U_\theta(\theta,\varphi)}{U_0} = \frac{4\pi r^2}{P_{rad}} \frac{\left|E_\theta(r,\theta,\varphi)\right|^2}{2\eta} \qquad [6.8]$$

The directivity according to φ is similarly defined. We will note that the directivity D is expressed as the additional contribution of the partial directivities:

$$D(\theta,\varphi) = D_\theta(\theta,\varphi) + D_\varphi(\theta,\varphi) \qquad [6.9]$$

In everyday language, when we mention the directivity of a radiation without specifying the observation direction, we mean in reality the maximum directivity of the radiation.

In reverberation chambers, in an ideal regime, there is neither a preferential polarization regime nor preferential incidence angle. We then estimate that the maximum directivity is that of an isotropic source ($D = 1$), and that the partial directivities are identical and thus equal to ½. Within this chapter we will come back to this point about the measurement of the total radiated power in reverberation chambers.

6.2.5. *Efficiency and gain of an antenna*

The directivity characterizes the angular distribution of the total power radiated by a source. However, we need to distinguish the radiated power from the power actually dissipated by the electric source, which is placed at the terminals of the antenna. In far-field, a radiation source is indeed comparable to an equivalent Thévenin generator, which is associated with its series impedance (R_S+jX_S), at the considered frequency of a continuous wave signal. This source of electromotive force V (see Figure 6.3) supplies the equivalent circuit of the antenna. We distinguish here the impedance of the antenna, whose real part (R_r) is made up of the

radiation resistance and a loss resistance R_l (both resistive or dielectric), as well as a reactive part (jX_r) which takes into account the energy possibly stored by the antenna.

The total radiated power is equivalent to the power dissipated by the radiation resistance of the circuit. The flow rate of the electromotive force in the inner resistance of the source corresponds to the radiated power. The radiated power is at a maximum when the internal impedance of the source is equal to the conjugate of the complex impedance of the antenna. This is only obtained at the tuning frequency of the antenna and this corresponds to $R_s = R_l + R_r$ and $X_s = -X_r$.

The total radiated power is then given by:

$$P_{rad} = \frac{R_r}{4} \frac{V^2}{(R_r + R_l)^2} \qquad [6.10]$$

$$P_S = \frac{V^2}{8(R_r + R_l)} \qquad [6.11]$$

The efficiency of the antenna is expressed as the ratio of the total radiated power to the power dissipated in the excitation source of the antenna. This quantity is denoted η_{rad}.

With the matching conditions of the antenna quoted above, we obtain:

$$\eta_{rad} = \frac{R_r}{R_r + R_l} \qquad [6.12]$$

The efficiency of the antenna is equal to the unit, when the R_l loss resistance vanishes and close to the unit, when we manage to make the radiation resistance sufficiently high compared to this loss resistance. The losses associated with the energy dissipation in an antenna are linked to the dielectric losses associated with the substrates and to the thermal losses (Joule effect). These thermal losses result from the non-perfectly conducting characteristic of the used materials.

Antenna efficiency is defined for a perfect matching. The global energy or power balance must also incorporate the matching factor of the antenna.

In other words, the P_S power considered here is not entirely the power supplied by the signal generator, according to the achievable matching level.

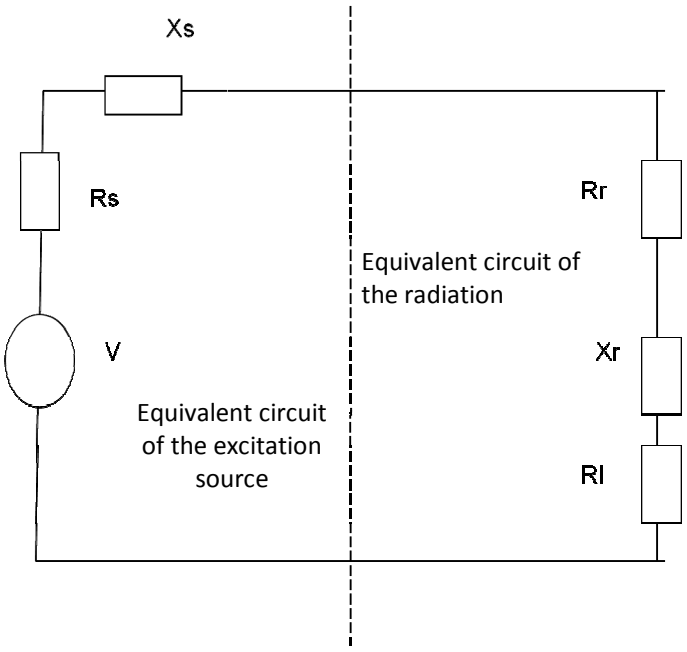

Figure 6.3. *Equivalent electric circuit of the radiation of an antenna*

The directivity is the angular distribution of the field independent from the ability of the antenna to radiate with low or high efficiency.

On the contrary, the notion of gain is linked to the power P_S supplied to the antenna:

$$G(\theta,\phi) = \frac{4\pi U(\theta,\varphi)}{P_S} \qquad [6.13]$$

Consequently, the gain is the product of the directivity by the efficiency of the antenna, whatever the considered direction of propagation:

$$G(\theta,\varphi) = \eta_{rad} D(\theta,\varphi) \qquad [6.14]$$

The gain (the directivity) is often used without specifying the radiation direction. We implicitly mean in that case the direction of the maximum of gain (or directivity).

6.2.6. *Effective area of an antenna*

The notions mentioned above have been presented in relation to a transmitting antenna. In the framework of the usual reciprocal propagation environments, the behavior of antennas is also reciprocal under the assumption of linear loads and these parameters are defined equally in transmission or in reception. The effective area of an antenna is a specific notion of the receiving antenna, otherwise very useful in the context of the measurement in reverberation chambers. The effective area of an antenna is the dummy surface that the antenna presents with regard to an incident plane wave. Given the effective area of an antenna in the direction of an incident plane wave of known power density, enables us to determine the received power at the input impedance of the antenna, when the latter is matched. This effective area is given by:

$$A_e(\theta,\phi) = \frac{P_{rec}}{dP_{inc}(\theta,\varphi)} \qquad [6.15]$$

In this expression, P_{rec} is the power dissipated on the matched load of the antenna. $dP_{inc}(\theta,\varphi)$ is the power density of a plane wave in Watt/m^2 incident on the antenna.

Let us consider two antennas at a far-field distance from each other. We are interested in establishing the power balance between a receiving and a transmitting antenna. The reciprocity principle implies that this power balance is identical whatever the choice of antenna for the transmission or the reception. This thus results in the following relationship, where the gain G_1 and G_2 of each antenna is considered in the direction of the other one:

$$G_1 A_{e2} = G_2 A_{e1} \qquad [6.16]$$

It is convenient to represent the effective area of any antenna with reference to a totally and ideally isotropic antenna. The effective area of an antenna in the considered direction of the incident wave is the product of the gain of this antenna in this direction by the effective area of an isotropic antenna:

$$A_e(\theta,\phi) = A_{e\_iso} G_e(\theta,\varphi) \qquad [6.17]$$

We can show [BAL 02] that the effective area of any antenna is finally put under the following form, by analytically calculating the radiation of a simple antenna (typically an elementary electric dipole):

$$A_e(\theta,\phi) = \frac{\lambda^2}{4\pi} G_e(\theta,\varphi) \qquad [6.18]$$

The possible omission of the incidence angles implicitly means that we consider the angle under which the effective area is at a maximum, unless otherwise specified.

6.2.7. *Transmission balance between two antennas – Friis expression*

From the reciprocity property, previously mentioned to justify the duality of the notions of gain and effective area of the antenna, the transmission balance as established by Friis [FRI 46] between a transmitting and a receiving antenna, can be directly established. More generally, this balance is established according to expression [6.19] giving the ratio of the power of the received signal, P_2, at the terminals of the receiving antenna and the transmitted power, P_1, at the transmitting antenna:

$$\frac{P_2}{P_1} = \frac{\lambda^2}{(4\pi d)^2} \eta_{ray\_1} \eta_{ray\_2} D_1(\theta_1,\varphi_1) D_2(\theta_2,\varphi_2) \left| \vec{\rho}_1 . \vec{\rho}_2 \right|^2 \qquad [6.19]$$

In this expression, we naturally find again the respective efficiencies of each of the antennas. The directivities of the two antennas are expressed in their local coordinate system and in the direction corresponding to where they are in line of sight to one another. In this expression, the unit polarization vectors of the radiation of each one of the antennas noted $\vec{\rho}_1$ and $\vec{\rho}_2$ also appear. The scalar product of these polarization vectors is equal to the unit, if the polarization of the transmitted wave corresponds to the polarization of the receiving antenna. However, in the case of polarization mismatch, this is the angle between the unit polarization vectors $\vec{\rho}_1$ and $\vec{\rho}_2$, which determines this transmission balance between two antennas.

6.2.8. *Formulation and properties of the radiation in a spherical graph*

6.2.8.1. *General expression of the electromagnetic field*

Knowledge of the general properties of electromagnetic radiation will be useful in section 6.6 of this chapter, which is devoted to the analysis of the radiated power in a reverberation chamber. The mathematical formalism, in its complete development for different spatial coordinate systems, can be found in reference books about antennas [BAL 02, ROU 86, STR 41].

However, we are devoting this section to the spherical coordinate system already used to describe the plane wave spectrum which results in the ideal random field distribution in a reverberation chamber. The electromagnetic radiation is controlled by Maxwell's equations and is produced by a current distribution. We assume this current of sinusoidal waveform and its distribution lies in a space restricted to a sphere of radius R_S. The upper case notation for the complex amplitude of harmonic signals is adopted in the following, such as for example for the electric field, $\vec{e} = \vec{E}\exp(-j\omega t)$. We then obtain:

$$\overrightarrow{rot}\vec{H} = -j\omega\varepsilon\vec{E} + \vec{J} \qquad [6.20]$$

$$\overrightarrow{rot}\vec{E} = j\omega\mu\vec{H} \qquad [6.21]$$

Thus, a waves equation in an electric field (as in a magnetic field) can be established in the form:

$$\overrightarrow{rot}\overrightarrow{rot}\vec{E} - k^2\vec{E} = \vec{J} \qquad [6.22]$$

The general form of the electromagnetic radiation can, however, be found by taking as a hypothesis the fact that we are only taking an interest in the field outside the zone where the source is.

Therefore, the propagation equation is reduced to:

$$\Delta\vec{E} + k^2\vec{E} = 0 \qquad [6.23]$$

We can show that equation [6.23] has, as a generic solution, the following vector functions $\vec{M}$ and $\vec{N}$:

$$\vec{M} = \overrightarrow{grad} f \wedge \vec{\vec{r}} \qquad [6.24]$$

$$\vec{N} = \frac{1}{k}\overrightarrow{rot}\vec{M} \qquad [6.25]$$

where f is a scalar generating function, i.e. a solution to the scalar wave equation:

$$(\Delta + k^2) f = 0 \qquad [6.26]$$

This generating function in a spherical coordinate system (r,θ,φ) can be obtained by the variable separation method, using expression [6.27].

The development briefly presented in this book is entirely presented in [HAN 88]. It is written in the form:

$$F_{mn}^{(c)}(r,\theta,\varphi) = A(m,n)z_n^{(c)}(kr)\overline{P}_n^{|m|}(\cos\theta)e^{im\varphi} \qquad [6.27]$$

with (*n*,*m*), a pair of integers taking any value so that $n \in [1,\infty[$ and $m \in [-n,n]$.

The $A(m,n)$ term represents a normalization coefficient given by:

$$A(m,n) = \frac{1}{\sqrt{2\pi}}\frac{1}{\sqrt{n(n+1)}}\left(\frac{-m}{|m|}\right)^m \qquad [6.28]$$

In this expression [6.27], the *c* exponent is associated with a family of generating functions, whose choice depends on the configuration of the electromagnetic problem set out. The c = 1 and c = 2 indices are in relation to the generating functions of a standing wave pattern and the c = 3 and c = 4 indices are relative to the generating functions of traveling waves. Thus, c=3 is associated with the propagation from the source towards infinity, i.e. a forward traveling wave, and reciprocally, c=4 corresponds to a propagation from infinity to the source, i.e. a backward traveling wave. For each one of the indices, the radial functions $z_n^{(c)}(kr)$ are as follows:

– $z_n^{(1)} = j_n(kr)$, where j_n is the spherical Bessel function;

– $z_n^{(2)} = n_n(kr)$, where n_n is the spherical Neumann function;

– $z_n^{(3)} = h_n^{(1)}(kr) = j_n(kr) + in_n(kr)$, where $h_n^{(1)}$ represents the spherical Hankel function of the first order;

– $z_n^{(4)} = h_n^{(2)}(kr) = j_n(kr) - in_n(kr)$, where $h_n^{(2)}$ is the spherical Hankel function of the second order.

In the expression of the generating function, the term $\overline{P}_n^{|m|}$ also appears, which is the associated and normalized Legendre polynomial expansion of degree *n* and of

order *m*. These polynomials play a central part in the description of the angular distribution of the radiated electromagnetic field.

We will come back to it in the next section, immediately following the development of the solution of the propagation equation.

Therefore, these generating functions, which are integrated into the second member of the solutions of waves equations [6.24] and [6.25], give:

$$\overrightarrow{M} = F_{1mn}^{(c)}(r,\theta,\varphi) = A(m,n)\begin{Bmatrix} z_n^{(c)}(kr)\dfrac{im\overline{P}_n^{|m|}(\cos\theta)}{\sin\theta}e^{im\varphi}\vec{\theta} \\ -z_n^{(c)}(kr)\dfrac{d\overline{P}_n^{|m|}(\cos\theta)}{d\theta}e^{im\varphi}\vec{\varphi} \end{Bmatrix} \quad [6.29]$$

$$\overrightarrow{N} = F_{2mn}^{(c)}(r,\theta,\varphi) = A(m,n)\begin{Bmatrix} \dfrac{n(n+1)}{kr}z_n^{(c)}(kr)\overline{P}_n^{|m|}(\cos\theta)e^{im\varphi}\vec{r} + \\ \dfrac{1}{kr}\dfrac{d}{d(kr)}\left\{krz_n^{(c)}(kr)\right\}\dfrac{d\overline{P}_n^{|m|}(\cos\theta)}{d\theta}e^{im\varphi}\vec{\theta} + \\ \dfrac{1}{kr}\dfrac{d}{d(kr)}\left\{krz_n^{(c)}(kr)\right\}\dfrac{im\overline{P}_n^{|m|}(\cos\theta)}{\sin\theta}\vec{\varphi} \end{Bmatrix} \quad [6.30]$$

By limiting ourselves in what follows to the description of the radiation of an antenna in free space, we can select as base functions, those relative to the c = 3 index in expressions [6.29] and [6.30], and we obtain for the electric field:

$$\vec{E}(r,\theta,\varphi) = k\sqrt{Z_0}\sum_{s=1}^{2}\sum_{n=1}^{\infty}\sum_{m=-n}^{n}Q_{smn}\vec{F}_{smn}^{(3)}(r,\theta,\varphi) \quad [6.31]$$

The F_{smn} functions, which are presented above, are orthogonal and orthonormal. Thus, a spherical wave of unit amplitude, according to any *s*,*m*,*n* triplet will have a radiated power of ½ Watt. Furthermore, in section 6.6 the index s will be related to the propagation of spherical waves under the TE and TM modes, respectively.

The total power radiated by a source located in free space, whose radiation will be previously established in the form of [6.31] will thus be given by:

$$P_{ray} = \frac{1}{2}\sum_{s=1}^{2}\sum_{n=1}^{\infty}\sum_{m=-n}^{n}\left|Q_{smn}\right|^2 \quad [6.32]$$

6.2.8.2. *Properties of electromagnetic radiation*

Thus, the electromagnetic radiation of any confined source is expressed in the form of a development in a series of orthonormal functions forming a vector space [6.31]. Therefore, the electromagnetic field is defined in a univocal way by a series of complex scalar coefficients Q_{smn}.

The $\vec{F}^{(3)}_{smn}(r,\theta,\varphi)$ basis functions of expression [6.31], on which the electromagnetic field is projected, have a radial component and an angular component that we observe in their expressions [6.29] and [6.30]. The angular distribution of the field relies, in reality, on the properties of the associated and normalized Legendre polynomials expansion $\overline{P}_n^{|m|}(\cos\theta)$.

More generally, the $\overline{P}_n^{|m|}(\cos\theta)e^{im\varphi}$ factor describes the angular distribution of the electromagnetic field. The $\vec{F}^{(3)}_{smn}(r,\theta,\varphi)$ basis functions are spherical harmonic functions based on these Legendre polynomials. Such polynomials of degree *n*, when restricted to the unit sphere, form a vector space of 2n+1 dimension (the *m* order varying from –n to +n). Development [6.31] is thus defined as a series expansion of spherical harmonics. These functions are naturally 2π periodic. The expansion in spherical harmonics resembles the Fourier expansion of the periodical functions. This is in fact its equivalence for the angular functions. Indeed, the $\overline{P}_n^{|m|}(\cos\theta)$ polynomials are in reality formed of terms made up of products of sinusoidal or co-sinusoidal functions of the angular variable $p\theta$, where *p* is an integer. Therefore, *p* determines the oscillating feature of the spatial distribution of these functions with regard to the polar angle. The number of transitions through 0 of a polynomial of degree *n* and of order *m* is *n-m*. Thus, the faster the angular variation of a radiation diagram is (what is called the spatial bandwidth of the radiation source), the more the basis functions on which the electric field is developed should be extended to a high *m* degree and/or a high *n* order.

If we take another look at the example of the elementary dipole in Figure 6.2, it has a very simple radiation pattern described by a $\sin\theta$ function. This is a function that goes only once through 0 for $\theta \in [0,\pi]$. A polynomial of degree 1 is sufficient to describe its radiation in reality. We show that in this case:

$$\vec{E}(r,\theta,\varphi) = k\sqrt{Z_0}Q_{201}\vec{F}^{(3)}_{201}(r,\theta,\varphi) \qquad [6.33]$$

Thus, only one mode is sufficient to describe the radiation of this elementary antenna. Observation of expression [6.30] shows that this mode is a direct function of the $\overline{P}_1^0(\cos\theta)$ polynomial, with $\overline{P}_1^0(\cos\theta) = -\sin\theta$. This quite simple configuration of the radiation is explained, in reality, by the elementary dimension of the considered antenna. The directivity of this antenna only reaches the value of 1.5. If, on the contrary, the considered radiating element has a higher dimension compared to the wavelength, then the expression of its radiation will require resorting to polynomial functions of higher degrees.

6.2.8.3. *Spherical waveguide and truncation of series expansion of spherical harmonics*

The radiation towards infinity of a source restricted to a sphere of radius R_s can be seen as the radiation existing in a spherical waveguide, whose dimension is R_s at the source location and endlessly increases. The modes of this waveguide are described by the harmonic functions introduced above. The $\overline{F}_{1mn}^{(3)}(r,\theta,\varphi)$ functions are TE modes, whereas the $\overline{F}_{2mn}^{(3)}(r,\theta,\varphi)$ functions are the TM modes for the calculation of the electric field. The radial nature of the propagation only depends on the *n* degree. In such a guide, some modes are evanescent, because the dimension of the guide is not large enough; on the contrary others propagate (with the evolution of the electric field in *1/r* in far-field). The propagation is maintained as long as the R_g radius of the guide meets the condition:

$$R_g > \frac{n}{k} \qquad [6.34a]$$

As long as the dimension of the source increases, i.e. when the ratio of the source dimension over the wavelength increases, the current distribution generating the field is likely to produce a higher variation of the angular field distribution and thus possibly a higher radiation directivity. The number of basis functions used to describe the radiation is a direct function of the radius R_s of the smallest sphere circumscribing the source. For the development exposed in [6.31], the summation indicated above is in principle infinite. However, for a source area restricted in a sphere of radius R_s, we can show [BUC 87] that this summation can be truncated to a $n \le N_{\max}$ value. $N_{\max}$ is the next upper integer (designated by n.u.i.) of the product of the wave number times the radius of the minimum sphere surrounding the antenna:

$$N_{\max} = n.u.i.(kR_s) \qquad [6.34b]$$

Limiting the development to this value enables us to describe the radiated field with a very reasonable approximation. The accumulation of the radiated power [6.32] up to this order, reaches the total radiated power at 1 or 2%. Only some aspects (such as for example the amplitude of the secondary radiation patterns) can require development at a higher order.

The measurements in reverberation chambers do not give access to the directivity. However, the properties of the electromagnetic radiation that we have just described enable us to estimate a possible order of magnitude, or at least a maximum bounding value of the directivity.

Before describing the transmission measurement methods specific to reverberation chambers, we come back to more conventional methods. Among these methods, the measurement in a spherical near-field test facility consists of measuring the tangential electric field on a sphere located in the Fresnel region of the radiation. This measurement enables us to calculate the Q_{smn} coefficients of the radiation, and from this, all its properties.

6.3. Measurement of the total radiated power in free space

6.3.1. *Definitions*

The total instantaneous power radiated by a device under test is defined by the integration of the flux of the instantaneous Poynting vector radiated through a surface surrounding the device. If this surface is the edge of a sphere surrounding the device set at its center, whose radius is long enough, then the flux through the surface according to all the directions of the space, is constant and represents the electromagnetic power actually radiated outside this surface. The radius of the sphere must be sufficient, so that only the electromagnetic field propagated by the source is thus quantified.

In principle it is in the Fraunhofer region that this condition is perfectly respected. It is only approximately respected in the part of the Fresnel region located at the border of the Fraunhofer region.

Thus, the total radiated power, which is evaluated below as a function of time, is expressed by the following relation:

$$P_{tr}(t) = \int_{\varphi=0}^{2\pi} \int_{\theta=0}^{\pi} \left(\vec{e}(t) \times \vec{h}(t)\right) \vec{u}_n \sin\theta d\theta d\varphi \qquad [6.35]$$

The $\vec{e}(t)\times\vec{h}(t)$ vector product is the instantaneous Poynting vector. Expression [6.35] is thus the flux of the Poynting vector through the surface delineating the sphere and in which the $\vec{u}_n$ unit vector appears, which is normal to this surface.

If during time, the evolution of the electromagnetic field is controlled by a pure harmonic source, then the electric field *e* and the magnetic field *h* can be written under the complex form, respectively $E\exp(j\omega t)$ and $H\exp(j\omega t)$, where *E* and *H* represent the maximum amplitudes of these harmonic signals.

With these notations, the total radiated power of a pure harmonic source is given by:

$$P_{tr}(f)=\frac{1}{2}\int_{\varphi=0}^{2\pi}\int_{\theta=0}^{\pi}\left(\vec{E}(f)\times\vec{H}(f)\right)\vec{u}_n\sin\theta d\theta d\varphi \qquad [6.36]$$

The objective of a measurement of total radiated power is most of the time to evaluate the spectral signature of the radiation. Analysis of the signal over time is favorable for the speed of the measurement. However, it assumes a very wide band receiver (oscilloscope), whose noise floor may be too high. On the contrary, however long it is, the measurement, with the help of a receiver centered on a tuning frequency combined with a filter with an adequate resolution bandwidth, enables us to evaluate the spectral response of the radiated electromagnetic power, by successively covering all the frequency range of interest. This second approach is favored by the standardization commissions, which we will tackle later on.

Measuring the total radiated power of a device at the frequency f_0 assumes that we can entirely collect this power through a measurement surface surrounding the antenna and previously defined. A preliminary condition must however be observed. At any point of the surface, the field must essentially be a radiation field at infinity. In other words, the imaginary field components stored around the radiating element must not be included in the calculation of the power actually radiated in the space. This fulfilled condition amounts to considering that the flux of the Poynting vector is a real scalar number.

If the surface is a sphere and the propagation medium is without loss, then this flux is conservative. In other words, if we have devices measuring this flux on the entire sphere surrounding the radiating element in the previously quoted conditions, then we measure the total radiated power of the device under test.

6.3.2. *Conventional measurement methods of the total radiated power*

One of most classical measurement methods consists of positioning the antenna under test in a far-field type test facility and acquiring the radiation diagram of the antenna with the help of an antenna calibrated in gain and in polarization. The power measured by the receiving antenna is recorded in a set of step positions describing the sphere at regular and sufficiently fine intervals.

In practice, we thus need to respect the Nyquist–Shannon sampling criterion, which states that such an interval must be lower than a distance of half the wavelength. This criterion is closely linked to the electromagnetic radiation properties, as they are presented in section 6.2 of this chapter. For a radiation source confined in a sphere of radius R_s, the N_{max} number necessary for the development of the electromagnetic field radiation fixes the sampling step according to the Nyquist-Shannon criterion. In order to correctly represent a function going through zero N_{max} times, we need to use at least N_{max} samples. This corresponds to a regular sample, so that:

$$\Delta\theta = \Delta\varphi = \frac{\pi}{N_{max}} \qquad [6.37]$$

We observe that this angular step corresponds to an arc of a circle of length $\lambda/2$ at the distance R_s. At the measurement distance R_{mea} higher than R_s, the arc of the circle corresponding to this condition [6.37], is $(R_{mea} / R_S)\lambda / 2$ length. The quality of the measurement notably relies on the calibration of the receiving antenna, whose gain and directivity must be known with high accuracy. The measurement of the power received by an antenna with excellent polarization purity enables us to retrieve the radiation pattern of the electric field on the whole sphere. The power measured at the terminals of the receiving antenna is indeed directly linked to the square of the electric field measured at a distance of the antenna, according to the far-field condition.

Alternately to the measurement in far-field, it is also possible to reach a specific evaluation of the total radiated power, if, nevertheless, the measurement distance is located in the Fresnel region (radiated near-field). We then show that probing the electric tangential field in amplitude and in phase on a sphere surrounding the antenna, is enough to describe the field in any zone of the space. This is in reality an application of Huygens' Principle.

Measurement of the electric tangential field on the measurement surface in two orthogonal polarizations, enables us to calculate the weighting (i.e. the Q_{smn} coefficients of relation [6.31]) of the basis functions, and therefore give access to the expansion of the field up to the order N_{max}. The field is thus mathematically

determined at any point of the space outside the measurement sphere, and the total radiated power is then easily calculable.

These techniques both use the sampled measurement of the electromagnetic field in all the directions of the free space, where the object is likely to radiate.

The characterization technique of the total radiated power in reverberation chambers is radically opposed of these conventional methods. Indeed, if a receiving antenna is also used, it collects power in a an arbitrary position and polarization. This is a set of measurements of this power during the electromagnetic stirring that we seek to link with the total power radiated by the device under test.

6.4. Measurement of the unintentional emission of a device under test

By unintentional emission, we mean any electromagnetic interference radiation produced by any electric or electronic device. We naturally seek to restrict the impact of these interference radiations by limiting them to acceptable levels.

We assume in what follows that the device under test, as well as the receiving antenna, are located in the working volume of the reverberation chamber. We also take a look at the radiation power when a steady state is installed in the reverberation chamber, i.e. in the radiation conditions of a pure harmonic signal or of a signal whose repetition frequency is high enough. The total power radiated by the device in emission is evidently the same as that involved in radiation conditions in free space.

Let us assume that the device radiates from the instant t = 0. The radiation will lead to the surface of the sphere Ω_e at the time $t_1 = R_e / c$, where R_e is the radius of the sphere and c is the speed of light. If this radius is chosen so that it satisfies the previously explained conditions, then it is possible in theory, to characterize the radiation properties of this device and notably the total radiated power. This would be possible with suitable probes positioned at the surface of this sphere and with an instrumentation enabling us to sense the temporal emission of the signals. Beyond the time t_1, the electromagnetic waves still propagate in the enclosure and it is then possible to link the answer of the probes to the only radiation of the device under test, up to the time t_2, from which a part of the radiated energy is once again intercepted via the surface of this sphere. Under these conditions, the total electromagnetic field is no longer the field diverging from the device. It also includes components of energy possibly converging once again on the device itself. Let us also note that this confinement of the energy in a reverberation chamber has opened an interesting prospect for the electromagnetic compatibility measurement linked to the use of the time reversal method [MOU 10].

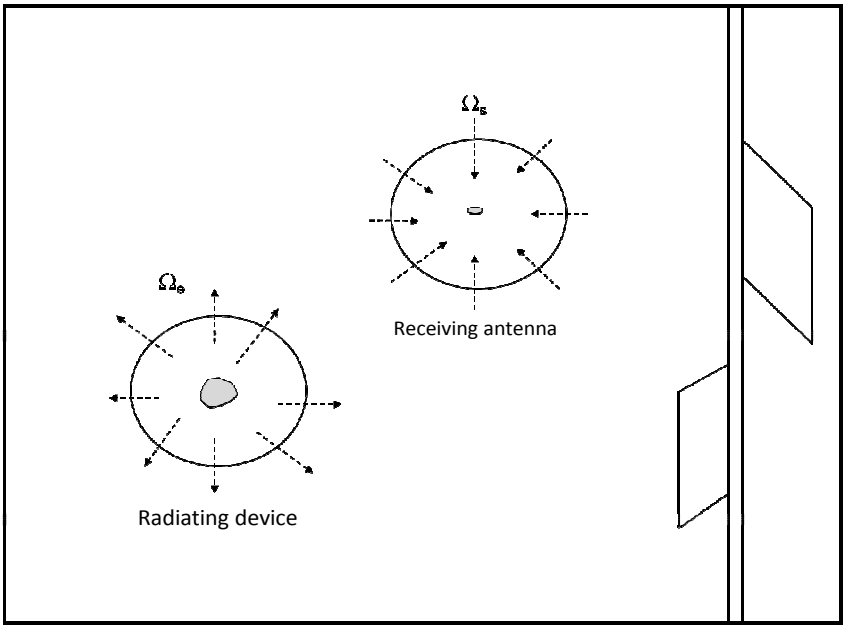

Figure 6.4. *Principle of the radiated emissivity test in a reverberation chamber*

The electromagnetic power transmitted to the reverberation chamber is thus the total radiated power from the device under test. By definition, the enclosure confines all of the electromagnetic energy thus transmitted by the device under test. If we continue the observation of the wave propagation throughout time, several phenomena will occur. The walls of the reverberation cavity are evidently responsible for this confinement, by reflecting a large part of the wave fronts that are incident to them. They also transform a part of this incident energy under the form of the Joule effect. As to the stirrer, also made up of metal materials, it contributes to these energy losses as well. As the multiple reflections of the wave fronts occur, the energy storage in the electromagnetic cavity manifests itself in the form of different propagation modes. Under the conditions of continuous emission of the source, the chamber reaches the steady state. For this regime, the stored energy in the chamber is constant and the different loss mechanisms involve power losses that all together balance the transmitted power from the device under test. Finally, as described in Chapter 4, the total radiated power in a reverberation chamber at equilibrium can be written in the form:

$$P_{tr}(f) = \sum_i P_{d_i}(f) \qquad [6.38]$$

The total radiated power is the sum of all the losses in the reverberation chamber in steady state. The losses in the reverberation chamber are naturally linked to the walls, which are made up of imperfectly conducting materials in the chamber, and to potential devices or objects also present in the cavity. They are also naturally linked to the device under test itself, which can absorb part of the electromagnetic energy that it generated. Finally, any antenna set inside the chamber also collects a fraction of the energy, which will mainly be dissipated by the charge of the receiver connected to it. By gathering the different terms of the losses, the expression of the total radiated power can be specified in the form:

$$P_{tr}(f) = P_{d\_mat}(f) + P_{d\_ant}(f) + P_{d\_ost}(f) \qquad [6.39]$$

In this expression, the loss factors have been gathered into three terms: the power losses in the walls P_{d_mat}, inside the device under test P_{d_ost} and in the receiving antenna P_{d_ant}. To lighten the notations in what follows, we will leave out the use of the frequency variable.

Thus, in steady state, the power received by the antenna under test is connected to the part of the total radiated power which was not dissipated by the materials of the chamber or by the device under test itself. However, at this stage of the reasoning, we have not yet brought into play any mode stirring mechanisms. Obtaining an ideally stochastic field is thus not completely guaranteed in these conditions. By assuming that the total radiated power is only carried by a limited number of modes, the resulting plane wave spectrum will include only a limited number of plane waves. Indeed, the power dissipated by a receiving antenna which is subjected to an incident wave in the (θ,φ) direction and with any polarization, can be obtained from the notion of antenna effective area, which is introduced in section 6.1 and more particularly by using expressions [6.15] and [6.18]:

$$P_{d\_ant} = \frac{\lambda^2}{4\pi}\eta_{ant}\int_0^{2\pi}\int_0^{\pi} D(\theta,\varphi)\, dP_{inc}(\theta,\varphi)\sin\theta d\theta d\varphi$$

$$P_{d\_ant} = \frac{\lambda^2}{4\pi}\eta_{ant}\int_0^{2\pi}\int_0^{\pi}\left\{\begin{matrix} dP_{inc\_\theta} D_\theta(\theta,\varphi) p_\theta(\theta,\varphi) + \\ dP_{inc\_\varphi} D_\varphi(\theta,\varphi) p_\varphi(\theta,\varphi) \end{matrix}\right\}\sin\theta d\theta d\varphi \qquad [6.40]$$

In this expression, the power density in the chamber is divided into two terms, according to two orthogonal field polarizations dP_{inc_θ} (according to θ) and dP_{inc_φ} (according to φ). The probability density function for the incidence angle

according to a given field polarization θ or φ, are designated by $p_\theta(\theta,\varphi)$ and $p_\phi(\theta,\varphi)$ respectively.

We saw in Chapter 2 (section 2.5), that the ideal random field produced in a reverberation chamber corresponds to the hypothesis of a spectrum with a large number N of plane waves of identical amplitude and a uniformly distributed polarization and random incidence angle. It results in:

$$p_\theta(\theta,\varphi) = p_\phi(\theta,\varphi) = \frac{1}{4\pi} \quad [6.41]$$

Let us assume that the receiving antenna has a linear polarization according, for example, to the polarization θ. This does not restrict the generality of the result. Therefore, from [6.40] and [6.41], we obtain:

$$P_{d\_ant} = \frac{\lambda^2}{4\pi}\eta_{ant}\frac{1}{4\pi}\int_0^{2\pi}\int_0^{\pi} dP_{inc\_\theta} D_\theta(\theta,\varphi)\sin\theta d\theta d\varphi \quad [6.42]$$

In the previous hypothesis of an ideal random field, the plane wave spectrum is uniform, thanks to the stirring process. The power density according to the polarization θ is thus identical to the power density according to φ, and thus equals half of the total power density dP_{inc}. The total power density is itself uniform for the entire angular spectrum. We finally deduce that:

$$P_{d\_ant} = \frac{\lambda^2}{8\pi}\eta_{ant} P_{inc} \quad [6.43]$$

In this last expression, the ½ factor is most commonly called the polarization mismatch factor in scientific literature. This term conveys the fact that an antenna polarized linearly in a reverberation chamber is only sensitive to the waves whose projection of the electric field vector on the polarization axis of the antenna is different from zero. This result is an essential consequence of the stochastic behavior of an oversized reverberation chamber, as described in Chapter 3 of this book.

Indeed, it appears that the power measured at the antenna loading impedance is completely independent from the directivity of the antenna. It is in reality only dependent on its efficiency and on its effective area corresponding to the effective area of an ideally isotropic antenna (expressions [6.17] and [6.18]).

The incident power on the antenna is not entirely (far from it) the total radiated power by the radiating device considered as an unintentional antenna. The dP_{inc} power density produced in the chamber is proportional to the total power radiated by the source, but is also lower when the energy losses in the walls and devices are high.

If we admit that the different losses globally gathered in expression [6.39] are independent of the radiation source, then a preliminary calibration process will enable us to access the estimate of the total radiated power according to a procedure similar to the one discussed later on in this chapter. If however, the losses associated with the device under test $P_{\text{d\_ost}}$ (or even $P_{\text{d\_ant}}$ if the device is an antenna) significantly intervene in the power balance, then the calibration process must be evidently matched. This will be the subject of next section.

The expressions that will be given in the next section reflect the behavior of an ideal reverberation chamber for which we directly access, and without error, the expected value of the observed magnitudes. In practice however, not only the chamber may not be so ideal but moreover, the quality of the total radiated power estimate also relies on the properties of the estimators of the moments of the power received by an antenna. This is naturally valid for the calibration stage of the losses of the test facility, as well as for the measurement of the total radiated power from the device. The uncertainty of this estimate is closely linked once again to the central limit theorem, which was outlined in Chapter 3.

6.4.1. *Calibration and evaluation of the total radiated power in reverberation chambers*

6.4.1.1. *Configuration of the calibration measurement*

The calibration method, such as was recommended for example in the EN 61000-4-21 standard [IEC 03], very strongly draws its inspiration from the method adopted for the calibration of the power collected at the input of a receiving antenna before carrying out a test in radiated immunity. This is about evaluating the insertion losses when the chamber is empty on the entire frequency of interest. These insertion losses represent the difference between the measured power on a receiving antenna which is placed in the chamber, and the power available at transmission, which is supplied by an antenna specifically used for this calibration. From expression [6.39], the I_{f} insertion losses can be expressed as:

$$P_{tr}(f) = P_{d\_ant}(f) + I_f \qquad [6.44]$$

These insertion losses can be evaluated in several locations with the help of a set of N stirrer positions and a repetition of the measurement in a set of P receiving antenna locations. If the antenna positions are chosen so that the distances between these positions are higher than the spatial correlation distance (Chapter 4, section 4.2.4), then we have P independent estimates of the moment of P_{tr}, which are calculated on N observations of the P_{d_ant} random variable. We will find a block diagram of this calibration method in Figure 6.5.

The estimate of the insertion losses must be brought back to the input power actually available, P_{disp} for the transmitting antenna. This input power is equivalent to the difference between the power of the forward traveling wave supplied by the RF source to the transmitting antenna and the power of the backward traveling wave linked to the mismatch of the antenna. This difference is in fact calculated on average during the stirrer rotation. Indeed, the standing wave regime generated in the reverberation chamber can really lead to a significant modification of its matching. Finally, the insertion losses I_f at the frequency f are calculated as follows:

$$I_f = \frac{1}{P}\sum_{p=1}^{P} I_f(P) \text{ , with } I_f(P) = \frac{\sum_{n=1}^{N} P_{d\_ant}^{[p]}(n)}{\sum_{n=1}^{N} P_S^{[p]}(n)} \qquad [6.45]$$

We find in this expression, the P_s term introduced in section 6.2, representing the power supplied to the used transmitting antenna. The choice of the number of stirrer positions N relies on the required level of uncertainty for the measurement. As far as electromagnetic compatibility measurements are concerned, the usual uncertainty for estimation of the total radiated power corresponds to the orders of magnitude usually expected in terms of EMC design: as an example, evaluating the total radiated power to + or -2 dB (i.e. from -30% to +50%), is a suitable estimate. This is of course quite insufficient in terms of performance characterization of intentionally radiating systems. We will take a look at this subject later on in section 6.7 of this chapter. Several tens of stirrer positions are really necessary for this estimate.

Indeed, the power measured at the receiving antenna input follows, in the case of an ideal stirring, an exponential distribution for which the standard deviation of the pdf is equal to its mean value. The empirical expectation of P_{d_ant} follows a normal distribution of $N(\mu, \mu/\sqrt{N})$ type, where μ is the rigorous mean value. For $N = 30$, the standard deviation of this normal distribution is of about 0.18. Thus, the estimate in only one position of the receiving antenna will be about +/- 35% for a

95% confidence interval. In the logarithmic scale this corresponds to an estimation uncertainty for P_{d_ant} of about 3.5 dB. This statistical uncertainty is probably acceptable from the point of view of EMC designers, since we are close enough to an acceptable approximation of the total radiated power. However, this is an evaluation of measurement uncertainty that concerns only this calibration stage. Indeed, the measurement process of the total radiated power relies on two estimates of the same type: the estimate of the insertion losses and the estimate of the total power radiated by the device under test.

In order to ensure an acceptable reproducibility level, the standardization commissions have thus recommended that this calibration process should be renewed for P positions of the receiving antenna. If we admit that this collection of measurements is formed of statistically independent implementations, then the uncertainty on the estimate of the power can be divided by the term $\sqrt{P}$. This point will be illustrated in section 6.5.

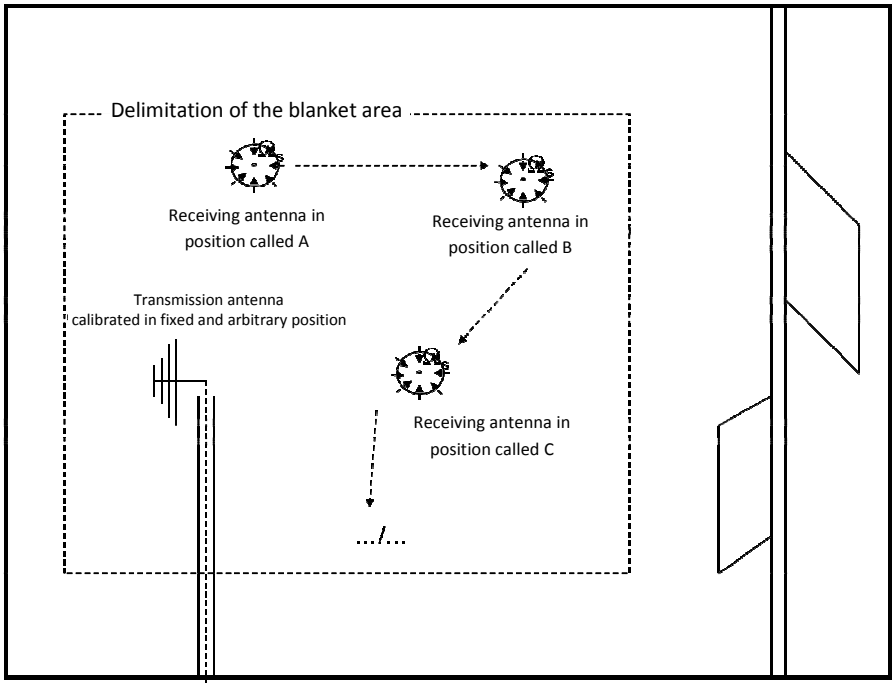

Figure 6.5. *Calibration of the measurement of the total radiated power with the help of two antennas. The measurement of the mean power received by the receiving antenna during a rotation of the mode stirrer, is renewed in several arbitrary positions A,B,C of the receiving antenna in the working volume of the chamber*

6.4.1.2. *Calculation of the total radiated power*

Measurement of the total radiated power is carried out by replacing the transmitting antenna, which allowed us to evaluate the insertion losses in the chamber with the device under test.

An important factor is involved in the balance of the power actually radiated in the reverberation chamber by the transmitting antenna: this is the efficiency of the antenna, which is defined in section 6.2 of this chapter. Indeed, the insertion losses characterize the ratio existing between the mean value of the signal collected on the receiving antenna and the signal supplied to the transmitting antenna. However, this transmitting antenna only partially converts the electric energy that is transmitted to it into electromagnetic radiation. The total power radiated by the transmitting antenna, which is used for the calibration, is thus given by:

$$P_{tr}(f) = \eta_{ant} \frac{1}{P} \sum_{n=1}^{P} P_S(P), with \qquad P_S(P) = \frac{1}{N} \sum_{n=1}^{N} P_S^{[p]}(n) \qquad [6.46]$$

where η_{ant} is the antenna efficiency of the transmitting antenna.

Let us replace the transmitting antenna that was used for calibration with the device under test. We seek to determine the total radiated power of this device at for a tuned frequency within the frequency band under investigation. By combining [6.44] and [6.46], we deduce that the total power radiated by a device replacing the transmitting antenna, could be given by:

$$P_{tr}(f) = \frac{\left\langle \frac{1}{N} \sum_{n=1}^{N} P_{d\_ant}(n) \right\rangle_R}{I_f \eta_{ant}} \qquad [6.47]$$

In this expression, the term at the numerator represents the mean value over R positions of the receiving antenna (this antenna is identical to the antenna used for the calibration) of the average power collected, on a set of N positions of the mode stirrer. The choice of the number of R positions is linked to the trade off between test time and uncertainty of evaluation, according to the trends mentioned above. The P_{d_ant} term corresponds to the measured power at the load impedance of the same receiving antenna as the one used during the calibration process.

If using a different antenna, we should also take into account the possible difference of efficiency between the two antennas.

If we come back to the expression of the balance of all losses in the chamber, we need at this stage to highlight a difficulty concerning the test procedure of the measurement of the total radiated power in a reverberation chamber. Writing [6.47] establishes that the total amount of losses in the chamber (expression [6.38]) has not been modified by the substitution of the transmitting antenna by the device under test. The incidence of this replacement is lower when the power losses in the antennas load impedance is low compared to the power losses through the walls, and when the device under test is made up of weakly absorbing materials. However, these two conditions are frequently not met. Consequently, it is necessary to impose a few additional precautions during the implementation of the test. We will summarize the entire applicable method in the following section.

6.4.1.3. *Operating mode of the measurement of the total radiated power in reverberation chambers*

We assume that the calibration of the empty reverberation chamber (i.e. in the absence of any device in the chamber, other than the pair of antennas necessary for the calibration) has been carried out conforming to the previous description.

6.4.1.3.1. Calibration check

Prior to the measurement itself, another stage is necessary. We can call it the calibration check. Then, we do not directly carry out a replacement: we need to add to the transmitting antenna (keeping its place in the reverberation chamber), the device under test, whose total radiated power we seek to measure. The device under test is not in operation. This device is thus not a source of electromagnetic radiation in this calibration phase. The measurement protocol of the calibration is then repeated, possibly for a more limited number of antenna positions. This economy can be justified if the insertion losses thus measured are of the same order of magnitude. We thus ensure, at least approximately, that the device under test does not significantly alter the power balance in the chamber. In the opposite case, the insertion losses I_f are re-evaluated in the presence of the device under test, for the same number of positions P of the receiving antennas, in order to reach an equivalent reproducibility level.

6.4.1.3.2. Determination stage of the total radiated power in reverberation chambers

The device under test is switched on and is operated as it would normally behave in real life conditions. The transmitting antenna used until then is no longer supplied, and thus, only the device under test is at the origin of the electromagnetic radiation in the chamber. To ensure similar power losses as during the calibration procedure, a 50 ohm coaxial resistance must be fixed at the antenna input port. Let us also note that this can have an influence on the low-frequency operating regime of a reverberation chamber, for which the quality factor of the antennas is potentially

low. Thus, the power losses in antennas constitute a significant amount of the total losses (i.e. transmitted power) in the chamber. This has been described in section 4.2.3 of Chapter 4.

It is then sufficient to replicate the measurement protocol of the calibration in R positions of the receiving antenna. The choice of the number of positions depends on the required reproducibility level. The higher the R number is, the more the measurement uncertainty is reduced. However, the chosen R number will not exceed the P number of positions chosen for the calibration.

6.4.1.3.3. Global statistical uncertainty

The global statistical uncertainty depends on the number of stirrer positions N and on the numbers *P* and *R* of antenna positions. The distribution of the resulting probability depends, in reality, on the ratio of the two power estimates, which are carried out during calibration and measurement. We have previously seen that the statistical uncertainty resulting from the estimate of the mean power, which is received during the calibration measurement, was inversely proportional to $\sqrt{NP}$.

A similar statistical uncertainty results from the measurement of the power received during the transmission of the device under test. It is inversely proportional to $\sqrt{NR}$. The global statistical uncertainty of this operation is thus linked to the ratio of the two random variables of normal distribution $N(\mu_2, \mu_2 / \sqrt{NR})$ and $N(\mu_1, \mu_1 / \sqrt{NP})$, with μ_1, the mean power received when the source is the transmitting antenna, and μ_2, the average power received when the device under test radiates. The final confidence interval (at 90%) is given by:

$$\frac{\mu_2}{\mu_1}\frac{(1-2/\sqrt{NR})}{(1+2/\sqrt{NP})} \leq \frac{\mu_2}{\mu_1} \leq \frac{\mu_2}{\mu_1}\frac{(1+2/\sqrt{NR})}{(1-2/\sqrt{NP})} \qquad [6.48]$$

In the hypothesis where R is chosen to be equal to P, the confidence interval of the estimate of the total radiated power is regardless enlarged, compared to that of a single measurement.

6.4.1.4. *Evaluation of the insertion losses on a very large frequency band*

The measurement of the unintentionally transmitted radiations most of the time assumes an analysis on various signal frequencies with some rules to determine the space between consecutive frequencies on a very large frequency spectrum. This naturally assumes in-depth knowledge of the evolution of the insertion loss *I*(*f*) as a

function of the radiation frequency. The selection of the tuned frequencies for evaluation of $I(f)$, and in particular the number of those frequencies and calculation of the frequency step, has a direct influence on the quantization of the dependence of the insertion losses, as a function of the frequency. The choice of a very small frequency step and thus of a large number of measurement frequencies has the effect of limiting the possible interpolation errors during the analysis of the radiation of the device under test, at frequencies other than those selected during the calibration. The bandwidth of the radio-frequency filter which is used in reception will also have to be identically fixed, for the calibration process and the test procedure. The parameters are set by the standardization commissions.

6.4.1.5. *Measurements based on the estimation of the maximum received power*

It is also possible to determine the total radiated power according to the evaluation of the maximum amplitude of the set of power data instead of estimating the mean value. The measurement procedure is exactly the same as already described. When the signal measured at the input impedance of the receiving antenna is on average only slightly greater than the noise floor of the receiver, the estimate of the mean is then altered by a bias linked to the insufficiency of the signal-to-noise ratio for the lower amplitudes of received power. The estimate of the maximum values is not however much altered by this bias and can turn out to be necessary. In the absence of this estimate bias, the mean value estimate is however preferable to the estimator of the maximum value.

If we admit that the exponential distribution of the power received on an antenna can be adopted in order to estimate the distribution of the maximum values (see Chapter 4 and notably the approximate expression [4.74]), then for the same number N of stirrer positions, the estimate of the maximum value presents a greater statistical dispersion than the estimate corresponding to the estimate of the mean value. Thus, for N = 30, the standard deviation brought back to the expectation of this distribution of the maximum is 32% according to [4.74] (against 18% for the standard deviation of the mean brought back to its moment). We also need to note that the expectation of the maximum increases with the number N of implementations. It is thus not appropriate to estimate the average power received in calibration and the maximum power received in the measurement phase of the device under test.

6.5. Measurement examples of the total radiated power

The measurement results presented in this section come from studies by the French working group PICAROS, gathering on the national scale, various academic and industrial actors around the subject of reverberation chambers.

The objective here is to illustrate the measurement method of the total radiated power in reverberation chambers, through the example of the measurement of the radiation of an autonomous source of the trade, which is usually used for the purpose of the calibration check of measurement facilities. This RF source is a periodical signal of 2 MHz fundamental frequency, with high order harmonics, and radiates via an antenna in a 80 MHz to 1 GHz bandwidth. The measurement method to be carried out aims at controlling the radiation of this source. In particular, it is important that the spectral analysis authorizes the distinction of each one of the tones of the discrete frequency spectrum. For this purpose, the resolution bandwidth of the analysis filter and the step between consecutive central frequencies, must be properly chosen. Choosing a frequency step lower or at worst equal to the resolution band of the used spectrum analyzer, ensures a global coverage of the frequency band.

6.5.1. *The calibration phase*

Prior to the measurement, the reverberation chamber will have been calibrated, so that the I_f coefficient should be actually known in the involved frequency band. Naturally, if need be, we will carry out the necessary interpolations during the measurement, if the value of this coefficient is known at the neighboring frequencies of the test frequency. In the example considered for this book, the calibration is carried out for 9 arbitrary positions of the receiving antenna (P = 9 in reference to the previous section). From a practical point of view, in order to increase the measurement speed, frequency sweeping on the whole band is carried out for every stirrer position. The data of all the measurements are stored and then processed later on. This naturally allows us to optimize the measurement duration, since only one stirrer rotation is carried out.

Figure 6.6 shows the I_f coefficient for each of these individual positions between the frequencies 600 and 650 MHz with a step of 75 kHz. The fluctuations are notably generated for neighboring frequencies of only a few hundreds of kHz. They show the stochastic nature of the measurement. The chamber used for this measurement is a chamber of about 90 m^3. These fluctuations are linked to the size of the set of data selected here, i.e. 60 positions of the mechanical mode stirrer. In this case, they can reach several dB.

The power measured by an antenna follows an exponential distribution, for which the standard deviation of the distribution is equal to its moment. The empirical estimate of I_f for each frequency of the measurement is thus a random variable, whose behavior is comparable to that of a normal distribution. The standard deviation of this normal distribution, around the rigorous mean, is in inverse proportion to the square root of the number of implementations or positions

of the mechanical stirrer, i.e. $1/\sqrt{60}$. We can then show that the expected range of fluctuations of this estimate will be located in theory, for an ideal random field, in a range of about 3.5 dB. The insertion losses naturally fluctuate in this frequency band, mainly due to two different mechanisms. Firstly, energy losses in the walls are proportional to the square root of the frequency. Secondly, the antenna effective area is itself proportional to the square root of the frequency. In theory the evolution of the losses thus follows a $f^{5/2}$ function. This only represents a fluctuation lower than 0.9 dB on the considered band.

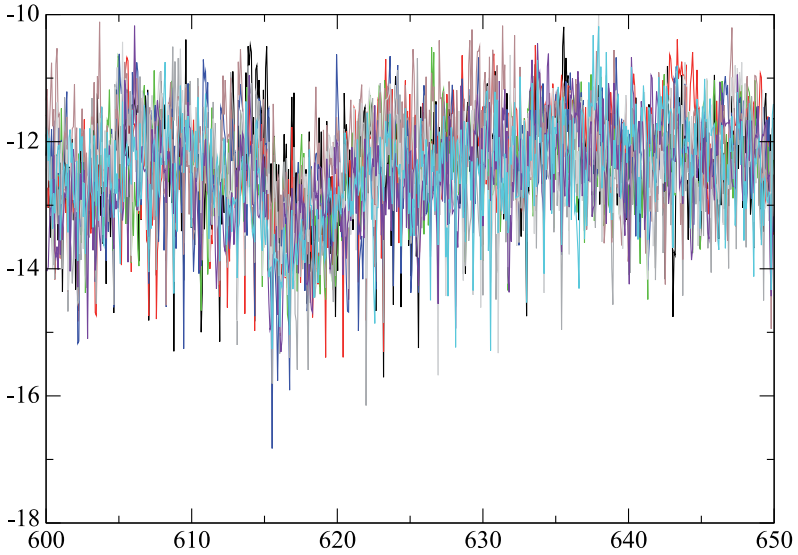

Figure 6.6. *Evolution of the insertion losses (10log I_β from 600 to 650 MHz in a reverberation chamber of 90 m^3. The nine curves shown are associated with the evaluation of this factor in 9 different and arbitrary positions of the receiving antenna in the chamber*

The advantage of a calibration in 9 positions lies within the fact that the insertion losses can thus be estimated with a reduced statistical uncertainty. Indeed, if we admit that each one of the 9 measurement samples is ideally independent because of a choice of receiving antenna positions, which minimizes the spatial correlation, then it comes down to estimating an empirical mean with 9 set of samples. The result is that the fluctuation of the mean on these 9 positions should be 3 times lower, by virtue of the central limit theorem. Under these conditions, the fluctuation range is reduced to about 1.1 dB.

Figure 6.7 shows the appearance of the small-scale fluctuations of the estimate of the clearly reduced insertion losses. The fluctuations on a larger scale can thus be allocated (notably around about 615 MHz) to fluctuations of the composite quality factor of the chamber. On the other hand, the measurements have been carried out with the help of antennas, in the current case of log-periodical type; whose efficiency is considered, in the absence of specific characterization, to be constant and equal to 0.75 for the entire frequency band considered. This rough estimate could also be at the origin of additional fluctuations.

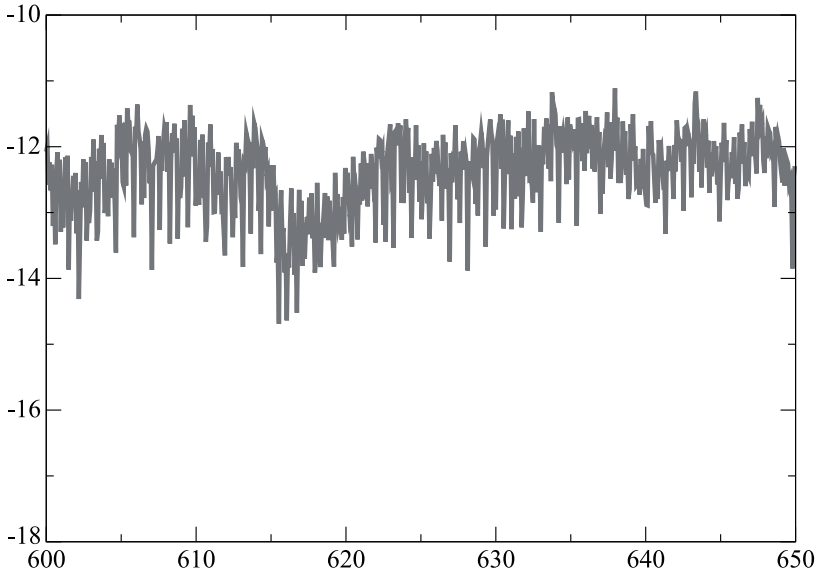

Figure 6.7. *Evolution of the insertion losses (10log I_ρ) from 600 to 650 MHz in a reverberation chamber of 90 m^3, which is evaluated according to the mean of the insertion losses, themselves evaluated on a set of 9 positions (see Figure 6.6)*

The curve given above is thus used as a reference, in the objective of determining the total power radiated by a device under test. From a practical point of view, we need to check that the residual fluctuation level is compatible with the reproducibility requirement of the test. From this point of view, the standards, notably the EMC standards, fix the acceptable uncertainty margins.

At this stage, it is important to make the difference between the calibration procedure and the test procedure, planned for example in a standardization framework. The calibration procedure is generally destined to be periodically carried out, such as is predicted for example by an insurance quality plan. We authorize in

general a longer procedure, which leads to a more precise estimate of the parameters of the test system, and more particularly here the insertion losses.

6.5.2. *The measurement phase of the device under test*

The receiving antenna used must be identical to the antenna used for the calibration. This is required by standardization commission. Beyond the fact it represents the simplest method, the purpose is to limit the uncertainty margin of the measurement. The purpose is also to recommend the antenna that was used for the calibration a long time ago. Indeed, the average power received by the receiving antenna depends on the modification of the reflection coefficient of the antenna in the chamber as well as on its radiation efficiency (term which by virtue of the reciprocity principle is defined as well in transmission or reception operation). Modifying this antenna would thus globally modify the quality factor of the reverberation chamber. But it is the same for the transmitting antenna, which contributed during the calibration, to the reception of a fraction of the power transmitted to the cavity by its intermediate. However, during the measurement phase, this is no longer this transmitting antenna, which is at the origin of the power transmitted to the chamber, but the antenna under test. So that the transmitting antenna preserves its own quality factor that primarily depends on its input impedance, we consequently need to cut off the excitation source of this antenna, while preserving the same load impedance which is classically matched to the antenna impedance. In practice, a coaxial load could replace the connection cable in the chamber, which is located between the source and the antenna. However, we note that the coaxial cable is also the locus of currents induced by the field distribution in the chamber and also contributes, even slightly, to the dissipation of a fraction of the total radiated power in the chamber. An additional precaution thus consists of loading the antenna at the level of the technical interface panel.

To carry out the test, we thus add into the chamber the device under test, whose radiation we seek to observe. As mentioned in section 6.4, the device can evidently take part in the modification of the global quality factor in the chamber, and consequently in a variation of the transmission balance between the two antennas by its own presence. Ideally, this could require renewing the complete calibration procedure presented in section 6.4.1.1. The purpose, in our particular example, is to examine the possible modifications of the level of the insertion losses measured in the empty cavity and presented in Figure 6.6. However, a partial check in only one position of the receiving antenna is favored, in order to make a rough but fast estimate of the losses, which are introduced by the device under test. This fast estimate is carried out to the detriment of the test accuracy, but the desired objective in this context was to reach a sufficient reproducibility level.

This check for the device, chosen here as an example, did not allow us to detect a modification of the mean value of the total power received by the receiving antenna in the presence of the aforementioned device. The reference curve for the calculation of the insertion losses thus remains identical to that determined during the periodical calibration phase of the chamber.

The measurement of the total power radiated by the device under test, consists of analyzing the response of the receiver, whose tuning frequency will be swept on the entire frequency band of analysis. The resolution filter will remain unchanged compared to the calibration process. However, the frequency step chosen for the sweeping, remains a function of the nature of the intrinsic quality factor of the radiations observed, when they are of narrow band type. It is however useless to use a discretization step lower than the $f / Q(f)$ ratio, where f is the working frequency. Indeed, in that case, it is quite difficult to discriminate the radiation spectral contributions of such close frequency, for which the answers of the chamber would be too much correlated. For more details, the reader can refer to Chapter 8 of this book for the study of the correlation of data with frequency for a reverberation chamber.

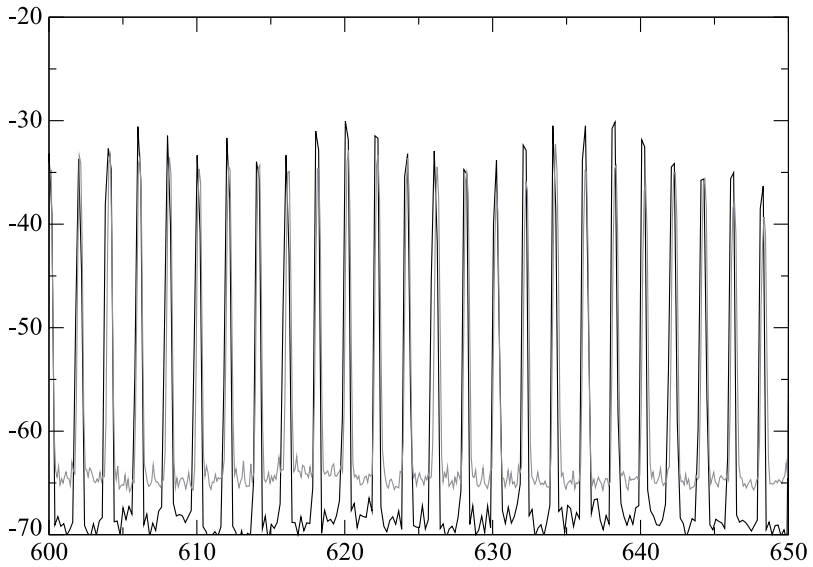

Figure 6.8. *Measurement example of the total radiated power (in dBm = 10logP(mW)) of a transmitting device from 600 to 650 MHz in two reverberation chambers of 40 m^3 and 90 m^3, which are evaluated for only one position*

Figure 6.8 has two measurement results for the device under test. They represent the total radiated power on the same bandwidth 600-650 MHz, which is recorded in two different reverberation chambers, of very different respective volumes, 40 and 90 m^3. For these two chambers, the same calibration and tests protocols were carried out for the same device. The objective of this comparison was to evaluate the test reproducibility from one chamber to another.

This radiation source manifests itself in the form of periodical signals forming a spectrum of lines spaced by 2 MHz, and whose spectral density is approximately constant on the observed frequency band. Between these equally spaced radiation frequencies, the measured signals approach the noise floor of the receiving system, whose level can naturally differ from one instrumentation to another.

We thus take a look at the amplitude of these lines and at the fluctuation of this amplitude as a function of the frequency. We notice that the two estimates are close to one another, differences reach only a maximum of about 4 dBm for the estimation of total radiated power. The fluctuations of the total radiated power for each one of the radiation frequencies are of the same order of magnitude as the fluctuations recorded between neighboring frequencies (small scale fluctuations) in Figure 6.6.

We recall here that the measurement of the device under test is only carried out for one position of the receiving antenna. In this case, the mean of the total radiated power is thus only estimated for 60 positions. We can estimate the theoretical order of magnitude of these fluctuations from expression [6.47] for $P = R = 1$ and $N = 60$. The confidence interval at 90% corresponds in that case to about 4.6 dB. This appears close to the level of the fluctuations actually recorded. Let us note that on the electromagnetic compatibility point of view, this result is considered to be useful enough, i.e. comparable to the uncertainty levels encountered for other test environments.

To conclude the description of this measurement method of the total radiated power in reverberation chambers, we need to point out that a clever method has been recently proposed [KRA 07] in order to evaluate the total radiated power of the device under test, without carrying out a preliminary calibration phase. This method consists of evaluating, at the same time, the contribution of the insertion losses and of the radiation transmitted by the device under test in the considered band, with the help of a pulse modulated sine signal analyzed with an appropriate resolution bandwidth of a spectrum analyzer, which is connected to the receiving antenna. The result is based on a time domain analysis, using a time sweep, the analyzer being tuned on the working frequency (“zero span” mode).

6.6. Total radiated power and radiated emissivity

The total radiated power can be considered as one of the possible physical parameters dimensioning the disturbing power of the device under test in its environment. However, we consider that this quantification is not enough, since the radiation directivity can be responsible for a significant increase in the power density transmitted in some directions of the space. This leads to a more important solicitation of possible electronic devices, which are located in these "favored" directions.

The conventional measurement of radiated emissivity generally has a characterization of the maximum radiation. The observation of this radiation is carried out at a standardized distance from the device under test, by successively placing an antenna in two orthogonal polarizations. The maximum of the received power is thus determined during the rotation of the device under test. This rotation, for practical reasons, is the most frequently carried out according to only one axis; the axis of a turntable, on which the device under test is placed. The test setup can also be completed by a highly conducting ground plane, which creates radiation interference. Therefore, the received signal is a function of the following parameters, the initial radiation pattern of the device under test, the receiver distance to the device, the heights of the device and receiver over the ground plane and naturally the interference transmission frequency. For more details readers can refer, for example, to the EN-55022 standard. From the designer's point of view, it would be interesting to determine an estimate of the directivity of the device under test, in addition to the characterization of the total radiated power in reverberation chambers. It would then become possible to estimate the maximum radiation in free space or according to a standardized process, such as the one that we have just briefly described.

However, the average power received by an antenna placed in an ideal reverberation chamber is in theory insensitive to the radiation pattern of the device under test. Two approaches are then possible. The first consists of trying to experimentally evaluate this directivity. Unfortunately, this approach comes down to using a more classical antenna measurement facility for a unintentionally radiating device. This is in theory possible, but requires us to resort to a test facility alternate to the reverberation chamber. On the contrary, the second approach consists of evaluating – at least approximately – the maximum expected directivity of a device mainly as a function of its size.

There are no rigorous methods allowing us to determine *a priori* the directivity of a radiating element, without carrying out a meticulous description of the topology of the circuits and materials constituting it. However, a few simple geometrical considerations enable us to evaluate a maximum bound of its directivity. This evaluation is very simple and deterministic: when this is about intentional

transmitters, and is more complex, when this is an unintentional transmitter, for which this maximum directivity is an estimate.

Electromagnetic radiation in space free of sources is a solution to the Helmholtz propagation equation, established from Maxwell equations. Readers wishing to go into depth on this theoretical question can refer to reference books in electromagnetic theory, notably [BAL 02, ROU 86, STR 41]. This propagation equation, recalled here once again, appears in the form:

$$\Delta\vec{E} + k^2\vec{E} = 0 \qquad [6.49]$$

Here it is represented in the form of an equation monitoring the behavior of the vector electric field $\vec{E}$. Its form is equivalent for magnetic field $\vec{H}$. This vector differential equation admits as a general solution, a set of functions forming a basis of orthogonal vectors. Thus, any solution of field $\vec{E}$, for any source, is given by an infinite set of weightings of these basis functions.

We have described these basis functions in section 6.2.7 for a spherical coordinate system (r,θ,φ). We have then established (see expression [6.31]) that the electric field (using the notation $\vec{e} = \vec{E}\exp(-j\omega t)$) radiating in free space outside a sphere of radius $R_{\min}$ surrounding the set of the radiation sources is given by:

$$\vec{E}(r,\theta,\varphi) = k\sqrt{Z_0}\sum_{s=1}^{2}\sum_{n=1}^{\infty}\sum_{m=-n}^{n} Q_{smn}\vec{F}_{smn}(r,\theta,\varphi), \forall r > R_{\min} \qquad [6.50]$$

In this expression, the orthonormal modal vector functions noted $\vec{F}_{smn}$ are the base of the functions, on which the complex coefficients Q_{smn} are projected. The $\vec{F}_{1mn}$ spherical wave vectors are associated with the transverse electric (TE) modes, and the $\vec{F}_{2mn}$ vectors are associated with the transverse magnetic modes. These modal functions depend on a radial propagation function (spherical Hankel function of the first order) and on the associated Legendre polynomial expansion of order n and of degree m describing the spatial physical structure of the modes, according to θ and φ angles respectively. An in-depth description of the properties of these functions can be found in [HAN 88].

Taken separately, each of the Q_{smn} coefficients raised to the square root represents the power of the radiation of the corresponding Q_{smn} mode. Although the modal series associated with equation [6.50] is infinite in theory, we show that this sum can be truncated, limited so that the total radiated power is approximately contained in all the terms of a truncated series at $n = N_{\text{tr}}$. This truncation is closely linked to the dimension of the radiating element and is given by:

$$N_{tr} = n.u.i.(kR_{\min}) + n_1 \qquad [6.51]$$

In this expression *n.u.i.* designates the next upper integer and n_1 is an integer number, whose value is fixed according to the experiment and to the desired measurement accuracy. We can show that the error committed on the determination of the radiation pattern and in particular for the main lobe of the latter, decreases very quickly with the increase of n_1 [BUC 87]. The maximum radiation directivity of an object can thus be evaluated by choosing $n_1 = 0$ in expression [6.51].

The directivity of the radiation in the (θ,φ) direction is given by:

$$D(\theta,\varphi) = \frac{\left|\sum_{s=1}^{2}\sum_{n=1}^{Ntr}\sum_{m=-n}^{n} Q_{smn}\vec{F}_{smn}(r,\theta,\varphi)\right|^2}{\sum_{s=1}^{2}\sum_{n=1}^{Ntr}\sum_{m=-n}^{n}\left|Q_{smn}\right|^2} \qquad [6.52]$$

We deduce [HAN 88] that the maximum directivity of an intentional transmitter, whose sources are inscribed in a sphere of radius R_{min}, is bounded, and this upper limit is given by:

$$D_{\max} = N_{tr}^2 + 2N_{tr} \qquad [6.53]$$

Thus, for electrically small structures such as $kR_{\min} < 1$, the maximum directivity evaluated by this expression is bounded to a value of 3. This approximately corresponds to a favorable radiation combination in phase, amplitude and polarization of two elementary electric and magnetic dipoles.

This expression of the upper bound of directivity generally leads to a high overestimate of this value, when we analyze the behavior in radiated emissivity of an unintentional source. This maximum bound of directivity produces an overestimation. The difference with the true maximum directivity is likely to be larger as the dimension of the device under test increases with regard to the wavelength. The bounded value of [6.53] becomes unrealistic for device dimensions of about a wavelength. The analysis proposed in [WIL 02] relies on the probability of uniform distribution of the radiation sources in the whole sphere occupied by the device under test. This hypothesis amounts to considering that every Q_{smn} weighting coefficient, more precisely each of the real and imaginary components of Q_{smn}, are random variables, according to a Gaussian process. The expectation of the upper bound of directivity is then given by the expression:

$$\left\langle D_{\max} \right\rangle = \frac{1}{2}\left[0,577 + \ln(N_S) + \frac{1}{2N_S} \right] \qquad [6.54]$$

with $N_S = 4\left(N_{tr}^2 + 2N_{tr} \right)$.

Thus, for a small size device under test ($kR_{min} < 1$), the bounding value of the directivity is estimated at 1.55. This approximately corresponds to the directivity of an elementary dipole.

These directivity estimates, for an intentional or an unintentional transmitter, are useful indicators for the determination of the nature of the disturbance risk in free space (or half-space) of a device, whose total radiated power has been characterized in reverberation chambers. It yields to a rough estimate of the upper bound of radiated electric field at a distance from the device under test, which is considered as a useful specification for electromagnetic compatibility.

6.7. Measurement of the efficiency and of the diversity gain of the antennas

It was recently proposed to use the reverberation chamber as a tool for measuring some antenna performances. We briefly mention here two possible applications of the previously described properties in terms of efficiency measurement and diversity gain of antennas. These aspects are briefly tackled here and deserve ampler developments. Readers can refer to the scientific literature for more details. Our objective here is to highlight the possible extension of the use of reverberation chambers.

6.7.1. *Measurement of the antenna efficiency*

The idea of measuring antenna efficiency comes from a very simple property. Indeed, the average total radiated power in reverberation chambers is directly proportional to the efficiency of the used transmission and receiving antennas. The first convincing results associated with this measurement in reverberation chambers are given in [ROS 01, ROS 02]. Assuming a continuous wave signal in steady state conditions, the balance of the transmitted power in the chamber can be put in the following form:

$$\left\langle P_{rec}(f) \right\rangle = \eta_{tra}(f)\eta_{rec}(f)\eta_{crbm}(f)\left\langle P_S(f) \right\rangle \qquad [6.55]$$

In this expression, P_S represents the output power of the amplifier or of the generator connected to the transmitting antenna. $<P_{rec}>$ is the mean of the power collected at the receiving antenna during the stirring process. This power is proportional to the efficiency of the transmitting or receiving antenna. Efficiency terms in equation [6.55] for the transmitting antenna $\eta_{tra}(f)$ and the receiving antenna $\eta_{rec}(f)$ account for the product of their antenna efficiency and their mismatch losses. The losses in the reverberation chamber are also transposed into an efficiency factor, noted η_{crbm}. Replacing the receiving antenna, whose efficiency must be perfectly known, with an antenna whose efficiency we seek to determine enables us to measure the unknown efficiency. The substitution of the receiving antenna is supposed to keep constant the total power losses in the reverberation chamber and the remaining antenna.

The measurement of the antenna efficiency requires, however, a large number of independent measurements to form an adequate sample, a much higher number than for the measurement of total radiated power. In this latter case, we aimed at determining the potential risk of disturbance brought by a device in electromagnetic compatibility. The order of magnitude of the number of measurements necessary in electromagnetic compatibility is several tens for an estimate of the total radiated power, with an uncertainty that we can determine according to the central limit theorem. Thus, under the assumption of an ideal random field distribution, the power received by a receiving antenna follows an exponential distribution, whose expectation is μ and the standard deviation $\sigma = \mu$.

The determination of an empirical mean on N measurements (or stirrer positions) thus follows a normal distribution centered on μ with a standard deviation $\mu / \sqrt{N}$. For a value of N = 50, the standard deviation of the corresponding Gaussian distribution is thus 14%. The antenna efficiency needs to be measured with an even greater accuracy, which assumes the use of several hundred measurements. The use of a mechanical mode stirrer cannot be sufficient and a mean evaluation on several measurement frequencies in the bandwidth of the antenna is required. Therefore, an accurate estimation of efficiency requires several samples of N collected at N stirrer positions. Frequency stirring is an adequate solution for this, providing that the quality factor associated with the reverberation chamber is high enough with regard to the antenna bandwidth. A small shift of frequency then allows a new set of uncorrelated data to be collected. Let us also note that an efficiency evaluation from the only measurement of the modulus and from the phase of the reflection coefficient (during the rotation of the mode stirrer) of the antenna placed in reverberation chamber was proposed in [HAL 01].

6.7.2. *Measurement of the diversity gain of the antennas*

Current telecommunication systems attempt to take advantage of the absence of a spatiotemporal correlation of the electromagnetic field, which is observed in some specific propagation channels. These phenomena are particularly visible when the power transmission between the transmitter and the receiver analyzes itself in the form of multiples paths. This diversity is used by combining, on the same receiver, several antennas placed at different points and possibly according to various polarizations. Thus, in specific time slots and position of the device supporting the antenna, when an antenna is poorly sensitive to the RF signal produced by the transmitting station, it is possible that another antenna collect a locally higher field level. The use of multiples antennas and adapted transmission algorithms are known by the name MIMO (multiple input – multiple output) techniques.

The performance of these systems depends on the propagation channel which may be very specific depending on typical distances of communication as well as on different types of outdoor or indoor environments. However, some of these propagation environments are comparable in reality to a plane wave spectrum (in azimuth) with an equal probability of the incidence angle of waves on the receiver. In this case, this propagation channel can thus be estimated by a Rayleigh distribution. This lead to the fact that the reverberation chamber can be a test tool in order to evaluate the provision of a multi-antenna configuration on a receiver.

[KIL 02, ROS 05] also proposed carrying out an evaluation of the diversity gain of the antennas in a Rayleigh channel which correspond to the distribution of the amplitude of a projection of the electric field ($\left|E_{x,y,z}\right|$) produced in a ideal random chamber The additional performance induced by the multi-antenna configuration is studied with reference to the probability density function of the power obtained by only one antenna. We define for example the diversity gain at the 1% quantile of the power distribution by:

$$G_{1\%} = \frac{P_{1\%}(f_{P\_N\_antennas})}{P_{1\%}(f_{P\_antenna\_single})} \qquad [6.56]$$

$P_{1\%}$ indicates the 1% quantile of the probability density of the associated power. The $f_{P\_antenna\_single}$ power density is empirically evaluated from the collection of the power measurements carried out during the stirring process on a single antenna. As a function of the nature of the definition of this diversity gain, we can set out to measure this antenna alone in free space, on the device itself, in the presence – or not – of other antennas.

The $f_{P\_N\_antennas}$ probability density is also empirically evaluated in reverberation chambers according, to the same stirring process as for the measurement of the single antenna. Each recorded value is this time made up of the value of maximum power recorded on one of the receiving antennas. Thus, the $f_{P\_N\_antennas}$ distribution shows a shift with respect to the distribution of a single antenna towards the highest power values. The increase of $P_{1\%}$ resulting from this is similar to the diversity gain. In fact, the empirical determination of the 1% quantile is rather estimated from the empirical cumulative distribution function.

As with the measurement of the antenna efficiency, the evaluation of the diversity gain, notably at relative power thresholds of about 1%, also requires a large number of implementations for a sufficiently accurate evaluation of this quantile. The same methods are used here: i.e. the combination of a mechanical stirring and the excursion on a frequency band in order to accumulate a sufficient set of data. The order of magnitude of the necessary sample size is about 1,000.

6.8. Discussion

6.8.1. *On the measurement of the radiated emissivity of a device in a reverberation chamber*

The reverberation chamber sets itself apart by the fact that it enables us to directly access, with a reasonable uncertainty in electromagnetic compatibility, the total radiated power. Some hypotheses about the nature of the radiating element (position and weighting of the complex amplitudes of the elementary sources equivalent to the device) are required in order to evaluate the directivity of the device. However, these elements only represent a probabilistic evaluation and are not measurable in reverberation chambers. All this shows however that the total radiated power is a significant and intrinsic feature of the device under test and may provide an interesting physical parameter, when analyzing the risk of interference caused by a source of electromagnetic radiation. With the knowledge of the total radiated power, the computation of a realistic upper bound of the power density radiated at a distance is readily available for devices with dimensions not exceeding the wavelength. Under these conditions, the link between the results obtained in reverberation chambers and by standard measurement means of the radiated emissivity in open space or in semi-anechoic chamber, can be established. In addition, we will note that the process used in open area test sites consists of measuring the radiation of the device, when it is installed on a ground plane and by only considering an azimuthal rotation of this device [IEC 08].

6.8.2. *On the measurements of radiofrequency devices in a reverberation chamber*

We have only presented an outline of what it is possible to characterize in reverberation chambers, from the point of view of the study of radiofrequency systems. Taking into account the different reverberation chamber properties that we presented, it is obvious that many other characterizations are possible. The control of the spectral power density occupied by a transmitter and the evaluation of the sensitivity level of a receiver are other potential examples. There is no doubt that such applications, with their specificities, could be the subject of detailed developments.

We have highlighted that the radiofrequency measurements set themselves apart in general from the EMC measurements, by their required precision. At first, this leads to the significant increase of the measurement times. On the other hand, this also leads to other methods of use of the reverberation chambers, combining for example mechanical stirring and the electronic stirring. However, we need to be cautious in terms of the estimate of statistical uncertainties. The ideality hypothesis of the random behavior of a reverberation chamber could be less acceptable, as soon as we take a look at several moments or quantiles of an empirical distribution. Thus, the study of the measurement uncertainty associated with each test procedure is a key element of the preliminary analysis, in order to guarantee a sufficient reproducibility level.

6.9. Bibliography

[BAL 05] BALANIS C., *Antenna Theory. Analysis and Design*, 3rd edition, John Wiley & Sons, Oxford, 2005.

[BUC 87] BUCCI O.M., FRANCESCHETTI G., "On the spatial bandwidth of scattered field", *IEEE Transactions on Antennas and Propagation*, vol. 35, no. 12, p. 1445-1455, December 1987.

[COR 76] CORONA P., LATMIRAL G., PAOLINI E., PICCIOLI L., "Use of a reverberating enclosure for measurements of radiated power in the microwave range", *IEEE Transactions on Electromagnetic Compatibility*, vol. 18, no. 2, p. 54-59, May 1976.

[FRI 46] FRIIS H.T., "A note on a simple transmission formula", *Proceedings of the I.R.E. and Waves and Electrons*, p. 254-256, May 1946.

[HAL 01] HALLBJORNER P., "Reflective antenna efficiency measurements in reverberation chambers", *Microwave and Optical Technology Letters*, vol. 30, no. 5, p. 332-335, September 2001.

[HAN 88] HANSEN W.W., *Spherical Near-field Antenna Measurements*, Peter Peregrinus Ltd, London, 1988.

[IEC 03] INTERNATIONAL ELECTROTECHNICAL COMMISSION, IEC 61000-4-21 Ed. 1.0, Electromagnetic Compatibility (EMC)-Part 4-21: Testing and Measurement Techniques – Reverberation Chamber Test Methods, 2003.

[IEC 08] INTERNATIONAL ELECTROTECHNICAL COMMISSION, IEC CISPR 22 Ed. 6.0, Comité International Spécial Perturbations Radioélectriques, Information Technology Equipment – Radio Disturbances Characteristics – Limits and Methods of Measurement, 2008.

[KIL 02] KILDAL P.S., ROSENGREN K., BYUN J., LEE J., "Definition of effective diversity gain and how to measure it in a reverberation chamber", *Microwave and Optical Technology Letters*, vol. 34, p. 56-59, July 2002.

[KRA 07] KRAUTHAUSER H.G., "On the measurement of total radiated power in uncalibrated reverberation chambers", *IEEE Transactions on Electromagnetic Compatibility*, vol. 49, no. 2, p. 270-279, May 2007.

[MOU 10] MOUSSA H., COZZA A., CAUTERMAN M., "Experimental demonstration of directive pulsed wavefront generation in reverberation chamber", *Electronic Letters*, vol. 46, no. 9, p. 623-624, 2010.

[ROS 01] ROSENGREN K., KILDAL P.S., CARLSSON J., LUNDEN O., "A new method to measure radiation efficiency of terminal antennas", *IEEE AP-S Conference on Antennas, Propagation for Wireless Communications*, Waltham, 2000.

[ROS 02] ROSENGREN K., KILDAL P.S., CARLSSON C., CARLSSON J., "Characterization of antennas for mobile and wireless terminals in reverberation chambers: improved accuracy by platform stirring", *Microwave and Optical Technology Letters*, vol. 30, no. 5, p. 391-397, Setptember 2001.

[ROS 05] ROSENGREN K., KILDAL P.S., "Radiation efficiency, correlation, diversity gain and capacity of a six-monopole antenna array for a MIMO system: theory, simulation and measurement in reverberation chamber", *IEEE Proceedings, Microwave Antennas Propagation*, vol. 152, p. 7-16, February 2005.

[ROU 86] ROUBINE E., BOLOMEY J.C., *Antennes: 1. Introduction Générale*, Masson, Paris, 1986.

[STR 41] STRATTON J.A., *Electromagnetic Theory*, McGraw-Hill, New York, 1941.

[WIL 02] WILSON P.F., HILL H.A., HOLLOWAY C.L., "On determining the maximum emissions from electrically large sources", *IEEE Transactions on Electromagnetic Compatibility*, vol. 44, no. 1, p. 79-86, February 2002.